ELSEVIER

Journal of Wind Engineering
and Industrial Aerodynamics 96 (2008) 713–735

JOURNAL OF wind engineering AND industrial aerodynamics

www.elsevier.com/locate/jweia

A brief review of recent results in vortex-induced vibrations

C.H.K. Williamson[a,*], R. Govardhan[b]

[a]*Fluid Dynamics Research Laboratories, Mechanical and Aerospace Engineering, Cornell University, Ithaca, NY 14853, USA*

[b]*Mechanical Engineering, Indian Institute of Science, Bangalore 560012, India*

Available online 6 August 2007

Abstract

In this brief review, we shall summarize fundamental results and discoveries concerning vortex-induced vibration, that have been made over the last two decades, many of which are related to the push to very low mass and damping, and to new computational and experimental techniques that were hitherto not available. We bring together new concepts and phenomena generic to vortex-induced vibration (VIV) systems, and pay special attention to the vortex dynamics and energy transfer that give rise to modes of vibration, the importance of mass and damping, the concept of a critical mass, the relationship between force and vorticity, and the concept of "effective elasticity", among other points. We present new vortex wake modes, generally in the framework of a map of vortex modes compiled from forced vibration studies, some of which cause free vibration. Some discussion focuses on topics of current debate, such as the decomposition of force, the relevance of the paradigm flow of an elastically mounted cylinder to more complex systems, and the relationship between forced or free vibration.

1. Introduction

Vortex-induced vibration (VIV) of structures is of practical interest to many fields of engineering. The practical significance of VIV has led to a large number of fundamental studies, many of which are discussed in the comprehensive reviews of Sarpkaya (1979), Griffin and Ramberg (1982), Bearman (1984), Parkinson (1989); in a book chapter by

*Corresponding author. Tel.: +1 607 255 3838; fax: +1 607 255 1222.
E-mail address: cw26@cornell.edu (C.H.K. Williamson).

0167-6105/$ - see front matter © 2007 Elsevier Ltd. All rights reserved.
doi:10.1016/j.jweia.2007.06.019

Anagnostopoulos (2002); and in books by Blevins (1990), Naudascher and Rockwell (1994), and Sumer and Fredsϕe (1997), and recently in the *Annual Review of Fluid Mechanics* by Williamson and Govardhan (2004). Here we focus on the more recent accomplishments of researchers, especially within the last decade. One stimulus for a resurgence of interest in VIV came from the Ocean Engineering Division of the US Office of Naval Research, which mounted a University Research Initiative and brought together many international researchers to work on common ground.

This review follows, and to some extent is an abridged version of, a more comprehensive review contribution, to which the reader is referred for more details, in the most recent *Annual Review of Fluid Mechanics* (Williamson and Govardhan, 2004). In both of these reviews, we are concerned principally with the oscillations of an elastically mounted rigid cylinder; with forced vibrations of such structures; with bodies in two degrees of freedom; with the dynamics of cantilevers, pivoted cylinders, cables, and tethered bodies. As a paradigm for such VIV systems, we shall consider here an elastically mounted cylinder restrained to move transverse to the flow. As the flow speed U increases, a condition is reached when the vortex formation frequency f_V is close enough to the body's natural frequency f_N such that the unsteady pressures from the wake vortices induce the body to respond. Certain wake patterns can be induced by body motion, whether the body motion is controlled or is free to vibrate due to the fluid forces. Williamson and Roshko (1988), studied the vortex wake patterns for a cylinder, forced to translate in a sinusoidal trajectory, over a wide variation of amplitudes (A/D up to 5.0) and wavelengths (λ/D up to 15.0). They defined a whole set of different regimes for vortex wake modes, in the plane of $\{\lambda/D,\ A/D\}$, where a descriptive terminology for each mode was introduced. Each periodic vortex wake pattern comprises single vortices (S) and vortex pairs (P), giving patterns such as the 2S, 2P and P+S modes, which are the principal modes near the fundamental lock-in region in Fig. 1. Visualization of the 2P mode is clearly presented in this figure also.

The 2P and P+S modes have been found in controlled vibration studies in-line with the flow (Griffin and Ramberg, 1976; Ongoren and Rockwell, 1988b), as well as transverse to the flow (see also Zdera et al., 1995). The P+S mode was also found in Griffin and Ramberg's (1974) well-known smoke visualizations. The significance of these modes from controlled vibration is that they provide a map of regimes within which we observe certain branches of free vibration. One deduction from the Williamson and Roshko study was that the jump in the phase ϕ of the transverse force in Bishop and Hassan's (1964) classical forced vibration paper, and also the jump in phase measured in Feng's (1968) free-vibration experiments, were caused by the changeover of mode from the 2S to the 2P mode. This has since been confirmed in a number of free-vibration studies (beginning with the pioneering work of Brika and Laneville, 1993), and we address this in Section 2. Such vortex modes occur for bodies in one or two degrees of freedom, for pivoted rods, cantilevers, oscillating cones, and other bodies. Response data from all of these studies have been correlated with the map of regimes described above.

Interestingly, a *forced* vibration can also lead to other vortex modes including a P+S mode, which is not able to excite a body into *free* vibration. In essence, a nominally periodic vibration ensues if the energy transfer, or work done by the fluid on the body, over a cycle is positive. This net energy transfer is influenced significantly by the phase of induced side force relative to body motion, which in turn is associated with the timing of the vortex dynamics. The problem of VIV is therefore a fascinating *feedback* between body

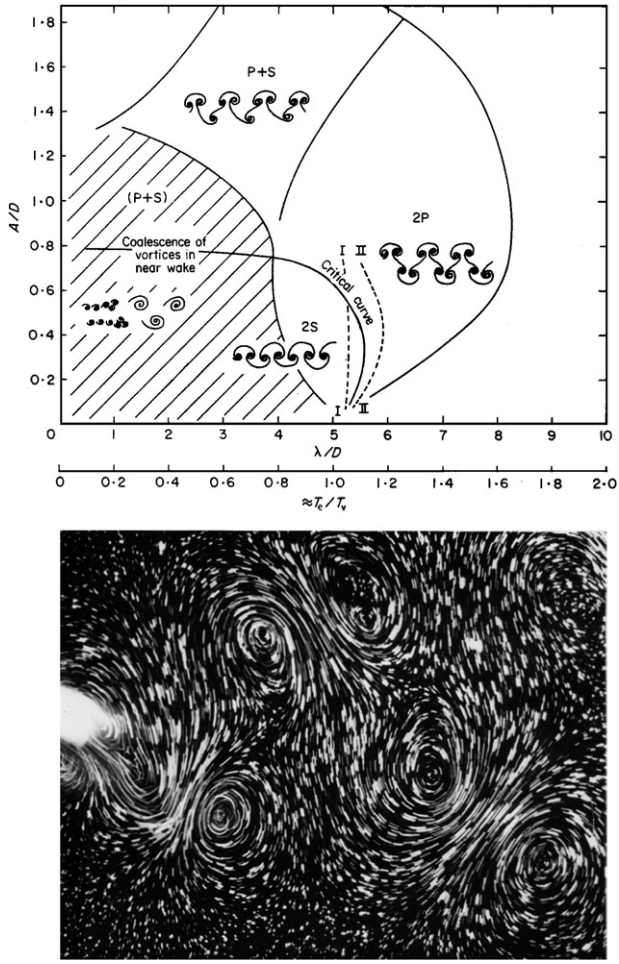

Fig. 1. The map of regimes for vortex wake modes (Williamson and Roshko, 1988), showing principally the 2S, 2P, and P+S mode regimes, which are relevant to the fundamental synchronization regime. The 2P mode, comprising two vortex pairs per half cycle, is visualized clearly below the mode map. Cylinder is towed through fluid in a sinusoidal trajectory to the left.

motion and vortex motion. In this review we shall therefore present not only response phenomena, but also the important vortex dynamics modes leading to the response.

Even in the simple case of the elastically mounted cylinder, many fundamental questions exist that are outstanding, for example: (a) What is the maximum possible amplitude attainable for a cylinder undergoing VIV, for conditions of extremely small mass and damping? (b) Under what conditions does the classically employed "mass-damping parameter" collapse peak-amplitude data? What is the functional shape for a plot of peak amplitude versus mass damping? (c) What modes of structural response exist, and how does the system jump between the different modes? (d) What vortex wake modes give rise to such structure dynamics? (e) What generic features can be discovered that are applicable to all VIV systems? To what extent are the enormous number of studies, for bodies

restricted to motion transverse to the flow, relevant to other, more complex VIV systems? (f) Because almost all of the studies of VIVs are at low and moderate Reynolds numbers, how do these results carry across to high Reynolds numbers?

Here we introduce an equation of motion generally used to represent VIV of a cylinder oscillating in the transverse Y direction (normal to the flow) as follows:

$$m\ddot{y} + c\dot{y} + ky = F, \tag{1}$$

where m is the structural mass, c the structural damping, k the spring constant, and F the fluid force in the transverse direction. In the regime where the body oscillation frequency is synchronized with the periodic vortex wake mode (or periodic fluid force), a good approximation to the force and the response is given by

$$F(t) = F_0 \sin(\omega t + \phi), \tag{2}$$

$$y(t) = y_0 \sin(\omega t), \tag{3}$$

where ω is $2\pi f$ and f the body oscillation frequency. The response amplitude and frequency may be derived in a straightforward manner from Eqs. (1)–(3), as done by several previous investigators. Here we formulate the equations in terms of a chosen set of nondimensional parameters, as in Khalak and Williamson (1999):

$$A^* = \frac{1}{4\pi^3} \frac{C_Y \sin\phi}{(m^* + C_A)\varsigma} \left(\frac{U^*}{f^*}\right)^2 f^*, \tag{4}$$

$$f^* = \sqrt{\frac{m^* + C_A}{m^* + C_{EA}}}, \tag{5}$$

where C_A is the potential added mass coefficient (taking the value 1.0), and C_{EA} is an "effective" added mass coefficient that includes an apparent effect due to the total transverse fluid force in-phase with the body acceleration ($C_Y \cos\phi$):

$$C_{EA} = \frac{1}{2\pi^3} \frac{C_Y \cos\phi}{A^*} \left(\frac{U^*}{f^*}\right)^2. \tag{6}$$

Quantities in the above equations are listed in Appendix A. Animated debate often surrounds the definition of "added mass" (C_{EA}) in these problems. Of course, it is not a true added mass, because it has a significant force component due to the vorticity dynamics. Note that the amplitude A^* in Eq. (4) is proportional to the transverse force component that is in-phase with the body velocity ($C_Y \sin\phi$), and, for small mass and damping, the precise value of the phase angle ϕ has a large effect on the response amplitude.

Feng (1968) contributed some important classic measurements of response and pressure for an elastically mounted cylinder. Fig. 2 presents his minimum-damping case, and it is apparent that there are two amplitude branches, namely the "initial" branch and the "lower" branch (in the terminology of Khalak and Williamson, 1996), with a hysteretic transition between branches. The mass ratio (or relative density) is very large because the experiments were conducted in air ($m^* \sim 250$). Much of the new work reviewed here comes from the push to much smaller mass and damping, generally using water as the fluid medium. Regarding the frequency response, the classical definition of "lock-in" or "synchronization" is often perceived as the regime where the frequency of oscillation (f),

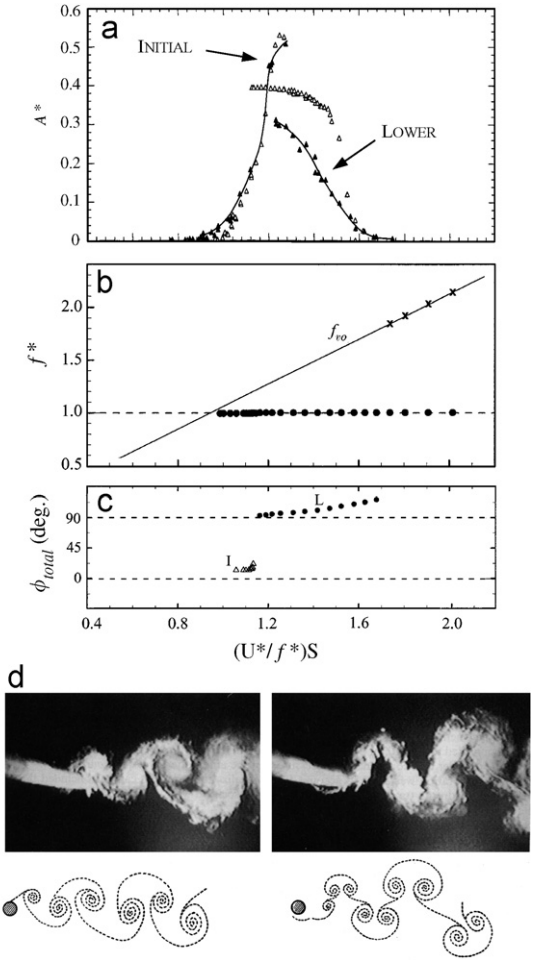

Fig. 2. Free vibration of an elastically mounted cylinder at high mass ratios. In (a), we compare the classical response amplitudes of Feng (1968) (*triangle symbols*), at the same ($m^*\zeta$) in air, with Brika and Laneville (1993) (*open symbols*); (b) and (c) show the vibration frequency and phase of the transverse force, as measured in water, but with the same $(m^* + C_A)\zeta \sim 0.251$ as used in the air experiments (Govardhan and Williamson, 2000). Brika and Laneville's smoke visualizations (d) showed for the first time that the response branches correspond with the 2S and 2P modes.

as well as the vortex formation frequency f_V, are close to the natural frequency f_N of the structure throughout the regime of large-amplitude vibration, so that $f^* = f/f_N \sim 1$ in Fig. 2(b). However, recent studies (in Sections 2 and 3) show a dramatic departure from this classical result; bodies can conceivably vibrate with large amplitude, at hundreds of times the natural frequency!

Feng also noted that the jump in response amplitude was reflected by a significant jump in the phase of the pressure fluctuations relative to body motion. One might suspect that a jump in phase angle (between transverse force and displacement) through resonance, as shown in Fig. 2(c), will be matched by a switch in the timing of vortex shedding. Zdravkovich (1982) showed this for the first time using visualizations from previous

studies. An excellent demonstration of this timing switch comes from the comprehensive forced vibration study of Ongoren and Rockwell (1988a). Gu et al. (1994) confirmed this from forced vibrations at small $A^* = 0.2$, in the ground-breaking first study of this problem using PIV.

2. Free vibration of a cylinder

Brika and Laneville (1993, 1995) were the first to show evidence of the 2P vortex wake mode from free vibration, using a vibrating cable in a wind tunnel. They stated that "the 2S and 2P modes can be clearly recognized, and the earlier explanation by Williamson and Roshko (1988) for the hysteresis loop in terms of a change in wake vortex patterns is confirmed". Fig. 2(d) shows their smoke visualization of these modes. They found a clear correspondence of the 2S mode with the initial branch of response, and the 2P mode with the lower branch.

Phenomena at low mass ratios and low mass damping are distinct from those mentioned above. A direct comparison is made between the response in water ($m^* = 2.4$) (from Khalak and Williamson, 1997b), with the largest-response plot of Feng conducted in air (Fig. 3). The lighter body has a value of $m^*\zeta$, around 3% of Feng's value, yielding a much higher peak amplitude. The extent of U^* over which there is significant response is four times larger than that found by Feng (an effect which was shown by Griffin and Ramberg, 1982). Although these are trends that might be expected, the character of the response for low mass damping is also distinct. The low-$m^*\zeta$ type of response is characterized by not only the initial branch and the lower branch, but also by the new appearance between the other two branches of a much higher "upper response branch". Khalak and Williamson (1996; 1997a, b; 1999) showed the existence of these three distinct branches, and using the Hilbert Transform to find instantaneous phase, force and amplitude, they were able to show that the transition between the Initial $\Leftrightarrow$ Upper branches is hysteretic, while the Upper $\Leftrightarrow$ Lower transition involves instead an intermittent switching.

The phenomenon of "lock-in" or synchronization (see Blevins, 1990; Sumer and Fredsøe, 1997), traditionally means that as the fluid velocity U^* is increased, a speed is reached at which the vortex shedding frequency f_V becomes close to the natural frequency of the structure (f_N), and the two frequencies synchronize. The shedding frequency and the oscillation frequency f remain close to f_N, and thus the ratio $f^* = f/f_N$ remains close to unity, as seen in Fig. 2 for high mass ratio. However, for light bodies in water, in this case for $m^* = 2.4$ in Fig. 3, the body oscillates at a distinctly higher frequency ($f^* = 1.4$).

Donald Rockwell's group at Lehigh University (see Gu et al., 1994) were the first to measure vorticity dynamics using PIV on the problem of controlled cylinder vibration. The first vorticity measurements for free vibrations, by Govardhan and Williamson (2000), confirmed that the initial and lower branches correspond to the 2S and 2P vortex wake modes (respectively), and these are illustrated in Fig. 4.

We mention here the important and much-debated question of "added mass". Lighthill (1979, 1986) discussed a formal decomposition of the total fluid force into its potential and vortex force components. As Lighthill put it, the "additional" vorticity ω_A, which contributes to the vortex force, refers to the entire vorticity in the flow field minus "part of the distribution of vorticity attached to the boundary in the form of a vortex sheet allowing exactly the tangential velocity (slip) associated with the potential flow". A full knowledge of the vorticity field would yield the vortex force through the concept of vorticity impulse.

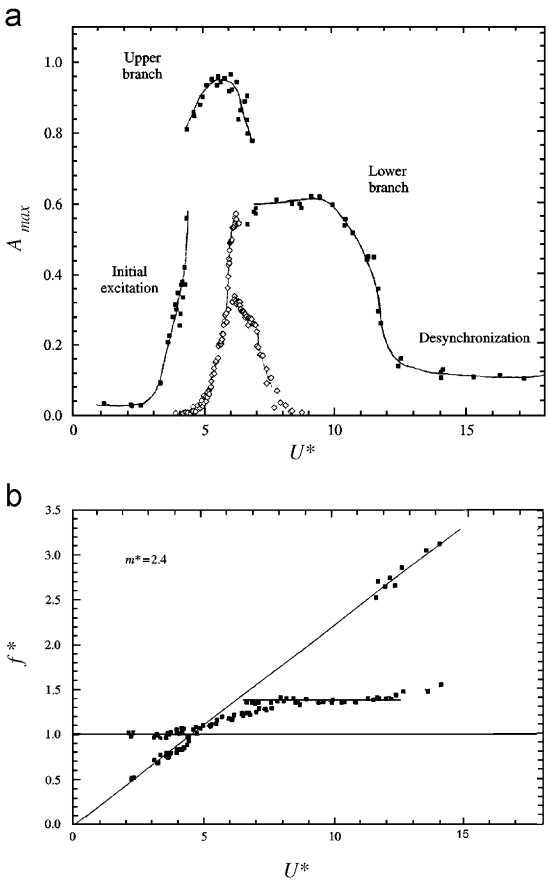

Fig. 3. Free vibration at low mass and damping is associated with the existence of an upper branch of high amplitude response, which appears between the initial and lower branches. The frequency of the lower branch is not close to the natural frequency, and is remarkably constant in (b). From Khalak and Williamson (1997b). Open symbols in (a) show the contrasting high-$m^*\zeta$ response data of Feng (1968).

As Koumoutsakos and Leonard (1995) wrote, the total force on a body (per unit length) in a viscous flow is given by

$$F_V = \rho \frac{d}{dt} \int (\omega_A \times x)\, dV + \frac{\rho \pi D^2}{4} \frac{dU}{dt}. \quad (7)$$

One of the more recent debates comes from the *BBVIV-2* Conference in Marseille, in June 2000 (see Leweke et al., 2001), which triggered much-needed clarification. Subsequently, Leonard and Roshko (2001) specifically discussed added mass of an accelerating body, defining it as "the impulse given to the fluid during an incremental change of body velocity, divided by that incremental velocity". They point out that such "properties of the added mass are well known from textbook derivations which are usually obtained for irrotational flow, and so it is not so well known that the resulting definitions are applicable more generally, e.g., in separated flows, such as those that occur in problems of

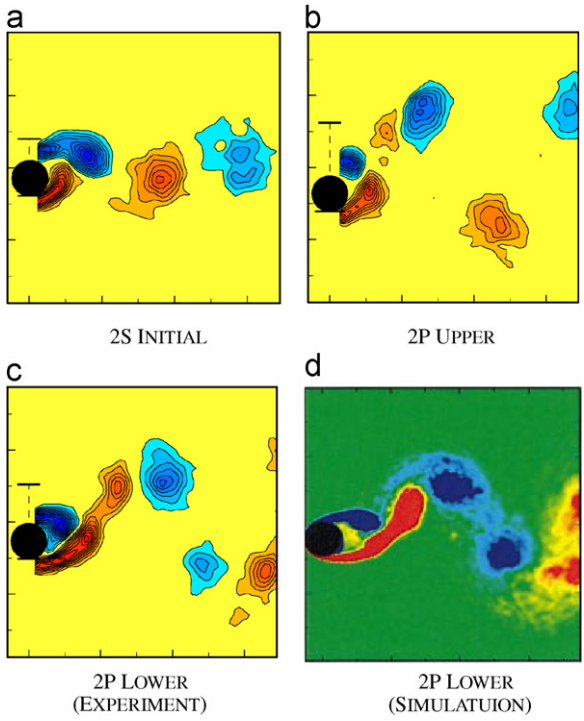

Fig. 4. Evidence from particle-image velocity vorticity measurements in free vibration that the initial branch corresponds with the 2S vortex wake mode, and that the upper and lower branches both reflect the 2P mode (Govardhan and Williamson, 2000). Blackburn et al. (2001) make a good comparison, computing the 2P mode of the lower branch, which is only possible with 3D simulations.

VIV. As a result, empirical relations are sometimes introduced into models, unnecessarily''. They provide a proof for the validity of the decomposition of the force in a general viscous flow.

Sarpkaya (2001) made a contrasting conclusion, stating that ''Lighthill's assertion that the viscous drag force and the inviscid inertia force acting on a bluff body immersed in a time-dependent flow operate independently, is not in conformity with the existing exact solutions and experimental facts''. Sarpkaya quoted an exact solution given in a really famous paper by Stokes (1851) concerning the force $F(t)$ on an oscillating sphere in a viscous fluid, valid for small amplitude. He presented that solution as his proof that ''it is impossible to decompose $F(t)$, for the flow under consideration, into an inviscid inertia force and a viscous force''. Sarpkaya concluded that such a force decomposition is equally impossible in the case of the transverse forces acting on bluff bodies undergoing VIV. It is of interest to note that his opinion is in direct disagreement with the evidence and analysis laid out by Leonard and Roshko (2001) and other references therein.

There have been excellent advances in the methods to measure induced force on a body, employing the concept of accurately measured vorticity impulse. Two research groups, one at Lehigh University and the other at Caltech, have been pushing forward these techniques, coupled with their expertize in PIV developments (Lin and Rockwell, 1996; Noca et al., 1999).

3. Existence of a "critical mass"

We see from several investigations that, as the structural mass decreases, so the regime of velocity U^* over which there are large-amplitude vibrations increases (see, for example, Fig. 3). Anthony Leonard indicated the large extent of such regimes for very low mass ratios, based on results related to numerical simulation, at the ONR Meeting at Brown University (June 1997). A surprizing recent result shows that the synchronization regime becomes *infinitely wide*, not simply when the mass becomes zero, but when the mass falls below a special critical value whose numerical value depends on the vibrating body shape.

The upper end of the synchronization regime for free vibration of a cylinder, with low mass damping, is generally distinguished by a lower amplitude branch, which has a remarkably constant vibration frequency f^*_{LOWER}, as typified by Fig. 3(b), and whose frequency level increases as the mass is reduced. Govardhan and Williamson (2000) presented a large data set for the lower branch frequency f^*_{LOWER} plotted versus m^*, yielding a good collapse of data onto a single curve fit based on Eq. (5):

$$f^*_{\mathrm{LOWER}} = \sqrt{\frac{m^* + 1}{m^* - 0.54}}. \tag{8}$$

This expression provides a practical and simple means to calculate the highest frequency attainable by the VIV system in the synchronization regime, if one is provided the mass ratio, m^*. An important consequence of Eq. (8) is that the vibration frequency becomes infinitely large as the mass ratio reduces to a limiting value of 0.54. Therefore, Govardhan and Williamson concluded that a critical mass ratio exists:

$$\text{Critical mass ratio } m^*_{\mathrm{CRIT}} = 0.54 \pm 0.02, \tag{9}$$

below which the lower branch of response can never be reached for finite velocities, U^*, and ceases to exist. These conditions are applicable for finite U^*/f^*, so when the mass of the structure falls below the critical value, one predicts that large-amplitude vibrations will be experienced for velocities U^* extending to infinity:

$$U^* \text{ end of synchronization} = 9.25\sqrt{\frac{m^* + 1}{m^* - 0.54}}. \tag{10}$$

This expression accurately marks the upper boundary of the shaded synchronization regime in Fig. 5(a). The fact that the critical mass turns out to be 54% is significant because it is in the realm of the "relative densities" of full-scale structures in engineering. We note carefully that this unique value of the critical mass is valid under the conditions of low mass and damping, so long as $(m^* + C_{\mathrm{A}})\zeta < 0.05$.

We note that added mass coefficients having a negative value can be observed in data sets from forced vibration (see Mercier, 1973; Sarpkaya, 1978; Gopalkrishnan, 1993) and in recent free vibration data sets (see Vikestad et al., 2000; Willden and Graham, 2001). The implications to free-vibration phenomena, such as the possible existence of a "critical mass", were not deduced in these works. However, it has generally been recognized that added mass (or C_{EA}) can predict possible free vibration frequencies.

There is nothing in principle to suggest that an experiment (consider the $m^* = 0.52$ case in Govardhan and Williamson, 2000) cannot reach $U^* \sim 300$, for example, at which point the system will vibrate vigorously at 32 times the natural frequency, $f \sim 32 f_{\mathrm{N}}$. This is far

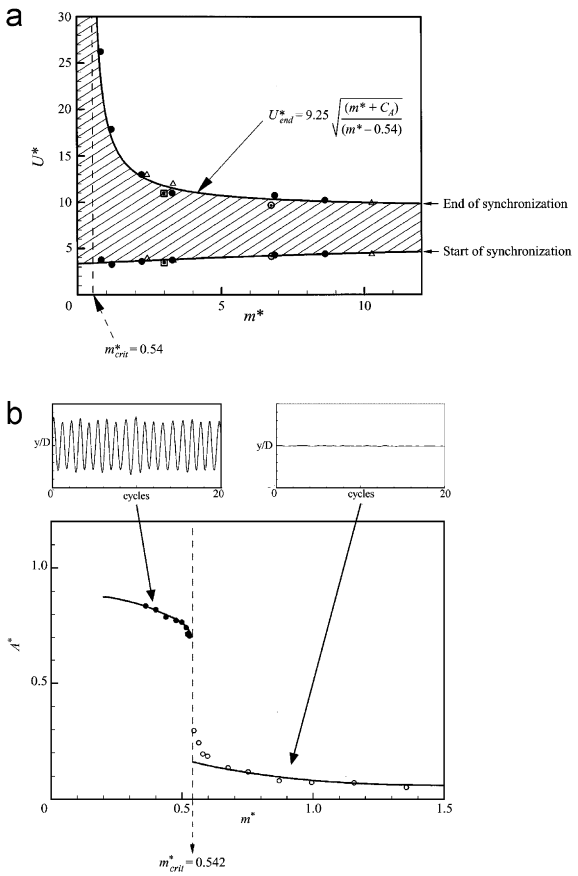

Fig. 5. Discovery of a critical mass. The synchronization regime of high-amplitude vibration (*shaded regime*) extends to infinite velocities as m^* approaches the value 0.54, in (a) (Govardhan and Williamson, 2000). The lower plot in (b), from an independent set of experiments at infinite U^*, shows that there is a sudden appearance of large-amplitude response when m^* just falls below 0.54 (Govardhan and Williamson, 2002). Symbols in (a) are: ●, Govardhan and Williamson (2000); △, Khalak and Williamson (1999); ▣, Hover, et al. (1998); ⊙, Anand and Torum (1985).

from the classical concept of synchronization, where resonant vibration is expected when the vibration frequency is close to the natural frequency, $f \sim f_N$!

It is possible, even within a laboratory, to take the normalized velocity U^* to infinity simply by removing the restraining springs, as done by Govardhan and Williamson (2002). In the experiments, a reduction of mass led to a catastrophic change in response; large-amplitude vigorous vibrations suddenly appear as the mass ratio is reduced to below a critical value, $m^* = 0.542$ (see Fig. 5(b)). This accurately proves the prediction of the earlier paper (Govardhan and Williamson, 2000); resonant oscillations persist up to infinite flow speeds, and in this sense the cylinder resonates forever!

How generic is the phenomenon of critical mass? Govardhan and Williamson (2002) deduced that it will be a universal phenomenon for all systems of VIV whose induced forces and dynamics are reasonably represented by Eqs. (1)–(3). In fact, one finds a critical mass, $m^* \sim 0.30$, for a tethered sphere system (Govardhan and Williamson, 2002), a critical

mass, $m^*\sim0.50$ for a pivoted cylinder (Flemming and Williamson, 2003), as well as $m^*\sim0.52$, in the case of an elastically mounted cylinder with two degrees of freedom (Jauvtis and Williamson, 2003c). Note that these values are valid for small mass damping.

4. The "Griffin" plot

An important question that has been debated for about 25 years is whether a combined mass-damping ($m^*\zeta$) parameter could reasonably collapse peak-amplitude data A^*_{max} in the Griffin plot. The use of a mass-damping parameter stems from several studies. Vickery and Watkins (1964), who considered an equation of motion for flexible cantilevers, plotted their peak amplitudes versus their *Stability parameter* $= K_S = \pi^2(m^*\zeta)$. Scruton (1965) used a parameter, proportional to K_S, for his experiments on elastically mounted cylinders that has since been termed the *Scruton number* $= Sc = \pi/2(m^*\zeta)$. A slightly different parameter was independently derived from a response analysis involving the van der Pol equation by Skop and Griffin (1973), and they compiled data from several different experiments as a means to usefully predict response amplitudes. The combined response parameter was subsequently termed S_G in Skop (1974), and is defined here as

$$\text{Skop}-\text{Griffin parameter} = S_G = 2\pi^3 S^2(m^*\zeta). \tag{11}$$

As a side note, the late Dick Skop (private communication) wrote to us stating that the well-known S_G initials actually represented the researchers "Skop" and "Griffin", a fact which is not generally known. Griffin et al. (1975) made the first extensive compilations of many different investigations, using S_G, and subsequently the classical log–log form of the plot (Griffin, 1980) has become the widely used presentation of peak response data. Despite the extensive use of the log–log Griffin plot by practicing engineers, it is not known precisely under what conditions the assumptions regarding U^*/f^* and f^* would hold, that would lead to a "unique" curve of A^*_{max} versus S_G.

Perceived problems regarding the validity of this widely used plot were pointed out repeatedly by Sarpkaya, in a large number of papers (see for example, Sarpkaya, 1978, 1979, 1993, 1995). He stated that simple observation of his equation of motion (equivalent to Eq. (1)) showed that "one must conclude that the dynamic response is governed, among other parameters, by m^* and ζ independently, not just by $(m^*\zeta)$". On the basis of the analysis of three data points, Sarpkaya (1978) suggested that one should use the combined parameter S_G only if $S_G > 1.0$, which rules out most of the plot, as one can see in Fig. 6.

On the other hand, Griffin and Ramberg (1982) performed two sets of experiments, each for the same value of $S_G = 0.5$–0.6, but with dissimilar mass ratios, $m^* = 4.8$ and 43. These data demonstrate two points. First, the lower mass ratio leads to a wider synchronization regime, extending over a larger range of normalized velocity U^*. Second, at the same S_G, the peak amplitude is roughly unchanged at $A^*_{max} = 0.5$, despite the fact that $S_G < 1.0$, thus disobeying the law stated above.

If we now plot an extension of the Griffin plot for a variety of experiments compiled by Skop and Balasubramanian (1997), but in this case using a linear Y-axis (rather than the classical log–log format) in Fig. 6(a), we see significant scatter, otherwise masked by the classical log Y-axis. Given this scatter, it does not appear reasonable to collapse data for such different VIV systems combined (free cylinder, cantilever, pivoted cylinders, etc.).

In Fig. 6(b) we present only those data corresponding to elastically mounted cylinders. Following Khalak and Williamson (1999), we introduce two distinct curves into the Griffin

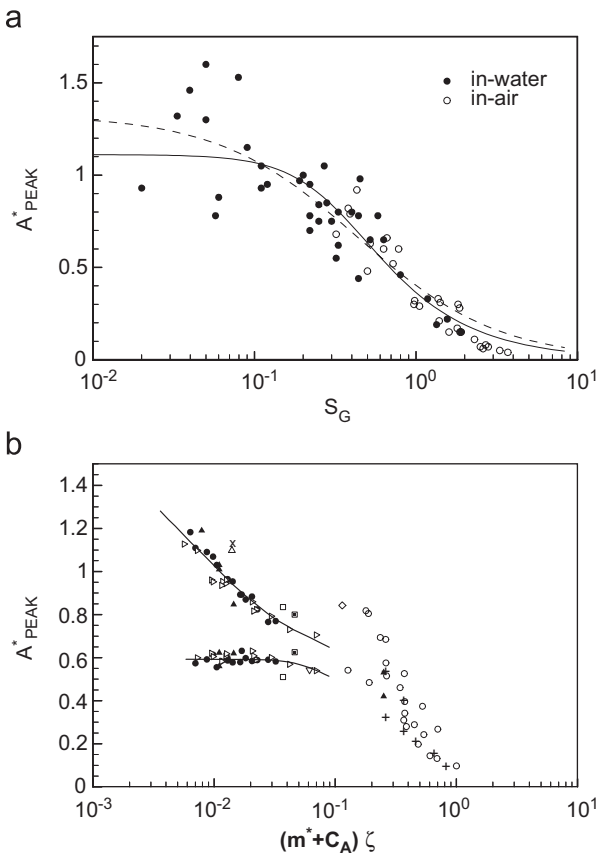

Fig. 6. The Griffin plot: (a) presents peak-amplitude data versus Skop–Griffin parameter S_G collected by Skop and Balasubramanian (1997), with more recent data, along with curve fits through the data. This indicates a large scatter. By removing those data for different vortex-induced vibration systems, in (b), one can demonstrate the reasonable collapse of data for elastically mounted cylinders (only). In (a), — is Eq. (16) with best-fit $B = 0.385$; $C = 0.120$. Symbols in (b) are: ●, Khalak and Williamson (1999); ▲, Govardhan and Williamson (2000); ▣, Hover, et al. (1998); ○, Griffin (1980); ▷, Jauvtis and Williamson (2003a–c); Δ, Moe and Overvik (1982); ▽, Angrilli et al. (1974); □, Owen et al. (2001); ◇, Gharib et al. (1998); +, Feng (1968); ×, Vikestad et al. (2000); ⊕, Anand and Torum (1985).

plot representing the peak amplitudes for both the upper and the lower branches. The resulting data from these diverse experimental arrangements appear to give an approximate functional relationship between A^*_{max} and $(m^* + C_A)\zeta$ over a wide range of parameters; applicable for the regime $m^* > 2$, and for $(m^* + C_A)\zeta > 0.006$. There seems to be a regime of validity for the Griffin plot that extends to two orders of magnitude lower mass damping (down to $S_G \sim 0.01$) than the limits ($S_G > 1$) suggested by Sarpkaya, and often quoted in the literature.

Finally one might observe in Fig. 6(b) that, even for the smallest mass damping, the peak amplitudes are not yet close to saturating at a specific value. One might ask: What is the maximum attainable amplitude that can be reached as $(m^* + C_A)\zeta$ gets ever smaller? The largest peak amplitude achieved so far in the Griffin plot is $A^* = 1.19$, but the trend of the

data suggests this is not the limit. One can conclude that, despite the enormous effort over the last 25 years to critique and define accurately this useful plot, it is not yet fully defined.

5. Forced vibration of a cylinder

One approach to predicting VIV has been to generate a complete experimental force data base by testing cylinders undergoing forced or controlled sinusoidal oscillations in a free stream. Several investigators, including Bishop and Hassan (1964), Mercier (1973), Sarpkaya (1978), Staubli (1983), Gopalkrishnan (1993), and more recently Hover et al. (1997, 1998), Sheridan et al. (1998), and Carberry et al. (2001, 2003, 2004, 2005), have measured the forces on bodies in harmonic, as well as multifrequency motion. Hover et al. (1997, 1998), in conjunction with Michael Triantafyllou's research group at MIT, developed an ingenious and extremely versatile experiment, namely a novel force-feedback "virtual cable testing apparatus". The system, mounted on a carriage over the MIT Towing Tank, comprises (a) a computer using a measured force signal from the test cylinder to drive in real time a numerical simulation of an equivalent mass-dashpot-spring system, and (b) a servomotor that imposes the computed motion to the submerged cylinder. The most recent contributions of this group are to push to much higher Reynolds numbers. The combined groups of Don Rockwell at Lehigh University and John Sheridan of Monash University recently made extensive measurements of force from controlled vibrations of cylinders, resulting in a number of very interesting papers (Sheridan et al., 1998 and Carberry et al., 2001, 2003, 2004, 2005). A summary of these and other new results can be found in the review of Williamson and Govardhan (2004).

6. *XY* motion of bodies

Despite the large number of papers dedicated to the problem of a cylinder vibrating transverse to a fluid flow (Y motion), there are very few papers that also allow the body to vibrate in-line with the flow. One principal question that may be posed is: How does the freedom to vibrate in-line with the flow influence the dynamics of the fluid and the structure?

In most past experimental work with XY vibrations (Moe and Wu, 1990, Sarpkaya, 1995), the mass ratios and natural frequencies were chosen to have different values, except for one data set for the same frequency in Sarpkaya. Under their chosen special conditions, these studies demonstrated a broad regime of synchronization, similar to Y-only studies, but with no evidence of the different response branches. Jeon and Gharib (2001) recently adopted a different approach, forcing a cylinder to move in the X and Y directions, in a fluid flow, under the prescribed motions given by $x(t) = A_X \sin(2\omega t + \theta)$; $y(t) = A_Y \sin(\omega t)$. Specific phase angles $\theta = 0^\circ$ and -45° were chosen. One of the most interesting results from the study of Jeon and Gharib is that even small amounts of streamwise motion ($A_X/A_Y = 20\%$) can inhibit the formation of the 2P mode of vortex formation.

Full-scale piles in an ocean current (Wooton et al., 1972), and similar cantilever models in the laboratory (King, 1974), vibrate in-line with the flow with peak amplitudes of the cantilever tip ($A_X^* \sim 0.15$). As Bearman (1984) and Naudascher (1987) noted, oscillations ensue if the velocity is close to $U^* \sim 1/2S$. King (1974) showed a classical vortex street (antisymmetric) pattern, although these investigators also discovered a second mode where the wake formed symmetric vortex pairs close to the body.

In most practical cases, cylindrical structures (such as riser tubes or heat exchangers) have the same mass ratio and the same natural frequency in both the streamwise (X) and transverse (Y) directions. Two recent arrangements that ensure such conditions are the air-bearing platform of Don Rockwell's group at Lehigh University (Leyva et al., 2007), and a pendulum setup at Cornell (Jauvtis and Williamson, 2003a–c). Both studies demonstrate a set of response branches, in contrast to previous XY experiments. Even down to the low mass ratios, where $m^* = 6$, it is remarkable that the freedom to oscillate in-line with the flow hardly affects the response branches, the forces, and the vortex wake modes. These results are significant because they indicate that the extensive understanding of VIV

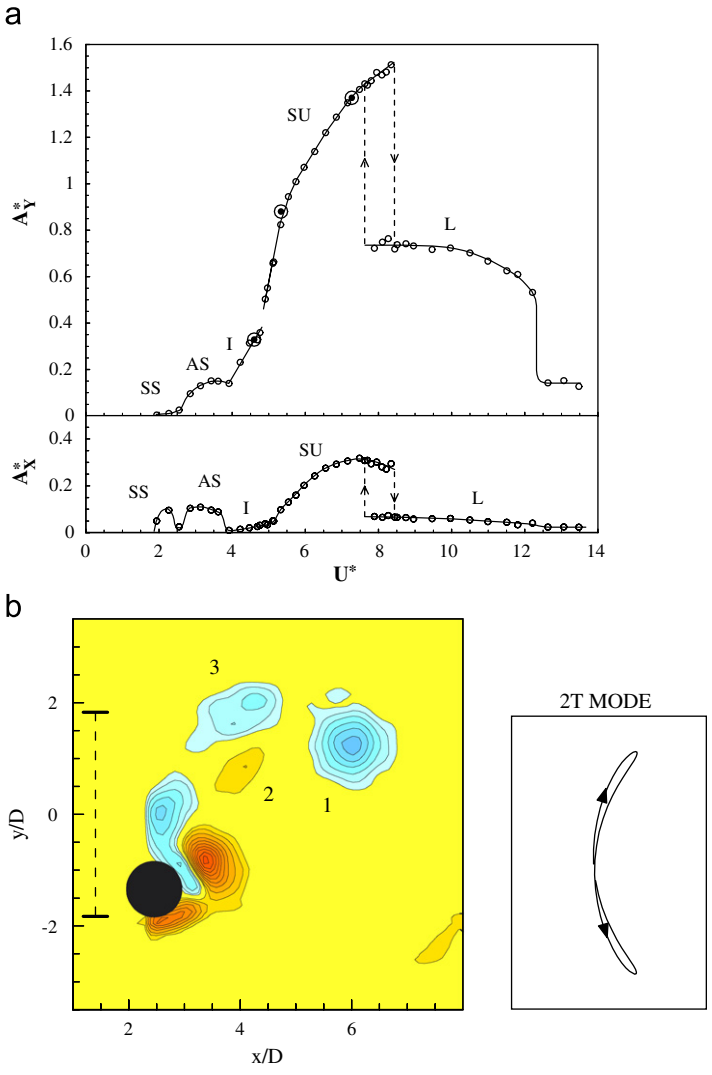

Fig. 7. Discovery of a "super-upper" branch of high-amplitude response that appears for XY cylinder vibration when mass ratios, $m^* < 6$. This corresponds with the appearance of a "2T" vortex wake mode, comprising a triplet of vortices to form in each half cycle. From Jauvtis and Williamson (2003b, c).

for Y-only body motions, built up over the last 35 years, remain strongly relevant to the case of two degrees of freedom.

However, there is a dramatic change in the fluid–structure interactions when mass ratios are reduced below $m^* = 6$. A new response branch with significant streamwise motion appears in what Jauvtis and Williamson (2003b, c) defined as the "super-upper" branch, which yields massive amplitudes of three diameters peak-to-peak ($A_Y^* \sim 1.5$), as seen in Fig. 7. This response corresponds with a new periodic vortex wake mode, which comprises a triplet of vortices being formed in each half cycle, defined as a "2T" mode following the terminology that Williamson and Roshko (1988) introduced.

7. "Complex flows": flexible, tapered, pivoted, and tethered bodies

As bodies become more directly practical, they generally become more complex, although many of the phenomena discovered for the simpler paradigm of the elastically mounted cylinder carry across to more involved structures, including those whose amplitude varies along the span. For example, in the case of flexible cantilevers, the recent work of Pesce and Fujarra (2000) and Fujarra et al. (2001) indicates that there is an initial branch of (tip) amplitude response, which has a hysteretic transition to a lower branch, similar to the elastically mounted or free cylinder. Techet et al. (1998) discovered a 2S–2P hybrid mode (shown in Fig. 8(a)), comprising the 2S and 2P modes occurring along different spanwise lengths of their tapered cylinder, with vortex dislocations between the spanwise cells. They showed an excellent correlation and prediction of these modes in the framework of the Williamson and Roshko (1988) map of modes.

VIVs of pivoted cylinders also exhibit similar branches of response to the cantilever and free cylinder, as seen from Balasubramanian et al. (2000) and Weiss and Szewczyk (2000), who studied many scenarios, comprising uniform and nonuniform cylinders in uniform or sheared flows. Voorhees and Wei (2002) observed some similar modes to those of the "free" cylinder (see also Dong et al., 2003), for their pivoted cylinder, and investigated the effects of spanwise flows. These studies confine vibrations to transverse motion, but Flemming and Williamson (2003) recently studied the case of a pivoted cylinder free to move streamwise as well as transverse to the flow. Over a range of body inertias I^* (equivalent to m^*), a number of different spanwise modes were discovered. For cases with high I^*, and negligible streamwise motion, either the 2S or 2P modes were observed along the span, but for lighter structures, the Techet et al. 2S–2P hybrid mode was found. Finally, Flemming and Williamson discovered a distinct new mode along the span, comprising two corotating vortices formed each half cycle, namely the "2C" mode, for the lightest of their structures.

Kim Vandiver at MIT has undertaken extensive field and laboratory experimental studies concerning cable dynamics (see for example, Vandiver, 1993; Vandiver and Jong, 1987), and he has developed a well-known cable VIV prediction program "SHEAR 7" (Vandiver, 2003) which is currently based on data for short laboratory cylinders. Related experiments have just been completed by Marcollo and Hinwood (2002), involving a cable in uniform flow, where they find evidence for similar added mass values and response branches as those found for short cylinders. Marcollo and Vandiver are presently undertaking high Reynolds number experiments in conjunction with a facility at Lake Seneca.

The group of George Karniadakis at Brown University have performed extensive computational studies, beginning with their studies to investigate laminar flow past a freely

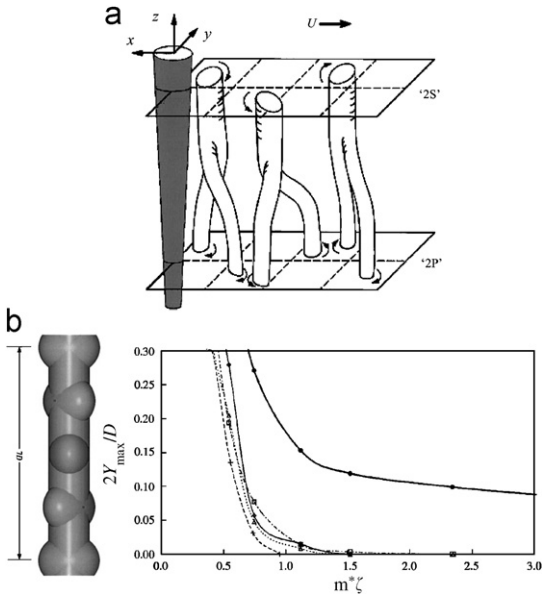

Fig. 8. (a) The Techet et al. (1998) "2S–2P hybrid" mode, comprising spanwise regimes of 2S and 2P modes, separated by periodic vortex dislocations, for a controlled transverse vibration of a tapered cylinder. (b) The "bumpy" cylinder of Owen et al. (2001) provides VIV suppression until a sufficiently low mass-damping ($m^*\zeta$) is reached when VIV resumes.

vibrating cable (Blackburn and Karniadakis, 1993; Newman and Karniadakis, 1997). The potential of three-dimensional computational studies is perhaps illustrated by the simulation in Fig. 9(a) showing the different types of vortex formation discovered at the nodes and antinodes of the cable undergoing standing wave vibration. Subsequent works (for example, Evangelinos and Karniadakis, 1999) developed a new class of spectral methods suitable for unstructured and hybrid grids. They computed a mixed response mode, comprising oblique and parallel shedding, caused by modulated traveling wave motion, whose effect on the lift force distribution has been studied. Lucor et al. (2001) investigated very-long bodies (aspect ratio > 500) in uniform and sheared flows to observe vortex dislocations of the kind found for fixed-body flows (Williamson, 1992), which cause substantial modulation of lift forces. Fig. 9(b) illustrates the intricate type of cable response, where the time history of the distribution of transverse displacement is exhibited, for a standing wave pattern in an exponential shear distribution.

Modeling the flow and vibrations of cables recently received a renewed interest. Triantafyllou and Grosenbaugh (1995) were able to usefully compute cable dynamics with an empirical model of the lift force as a linear function of the amplitude. Skop and Balasubramanian (1997) and Skop and Luo (2001) undertook extensive modeling of spanwise vortex shedding and structure dynamics of cylinders in uniform and sheared flows using van der Pol type oscillators, with a coupling term proportional to body velocity.

In a systematic paper, Facchinetti et al. (2004) concluded that the optimal coupling term involves the body acceleration, rather than the displacement or velocity. This is a useful result for future modeling developments. Facchinetti et al. (2004) also looked into the

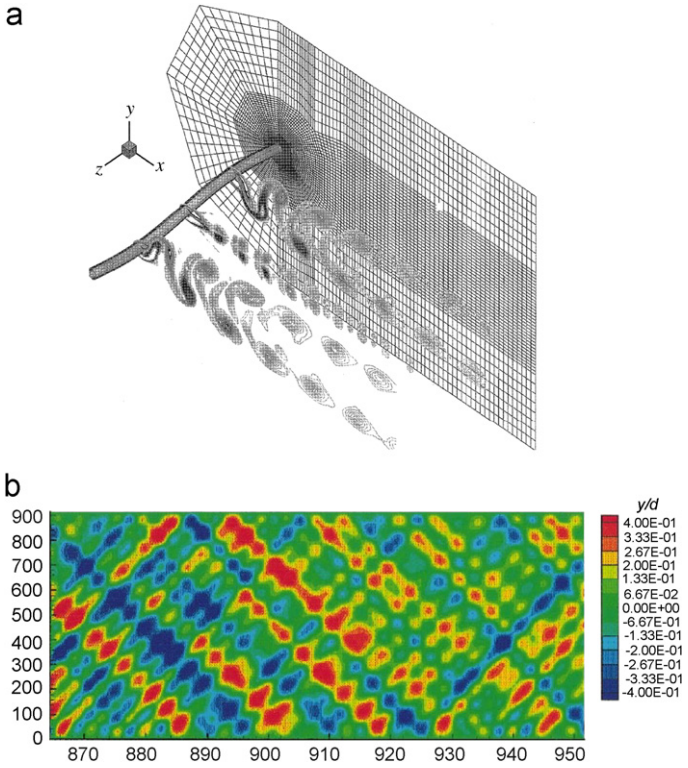

Fig. 9. Three-dimensional computations of vortex-induced vibration of a flexible cable are now possible; here we see wake vortex dynamics at nodes and antinodes of a cable vibrating with a standing wave (Newman and Karniadakis, 1997, 1996). Further results from the research group at Brown University (Lucor et al., 2001) show contours of transverse amplitude along the span of a cable (*vertical axis*) as a function of time (*horizontal axis*), for a cable undergoing a mixed response of traveling and standing waves.

problem of vortex-induced waves, which they labelled "VIW", using both their modeling approach and also experiment. Kim and Perkins (2002) studied other cable models, showing the essential character of experimental VIV response, including hysteresis. Finally, the approach of Willden and Graham (2001) is unique in that they developed an efficient "quasi-3D" simulation, where the two-dimensional flow is computed at various spanwise locations, and these are linked by a three-dimensional large-scale vortex lattice representation.

Recent investigations to suppress VIV stemmed from the original work of Tombazis and Bearman (1997) and Bearman and Owen (1998), where they investigated the influence of an imposed spanwise waviness of the flow separation lines around bluff bodies. They achieved a drag reduction of 30% and a suppression of classical vortex shedding. A principal idea is to weaken vortex shedding without the drag increase associated with traditional "helical strakes" (Zdravkovich, 1981). Subsequently, Owen et al. (2001) studied the effects of a sinuous waviness to the axis of a cylinder, as well as the effects of introducing hemispherical bumps to the cylinder surface, which yield an encouraging 25–47% reduction in drag. These methods diminished the value of mass damping below which vibrations set in, as shown in Fig. 8(b), but have not completely eliminated the

problem of VIV. Introduction of trip wires by Hover et al. (2001) have also diminished the response magnitude and regime of lock-in for VIV.

8. Concluding remarks

In this review, we discuss many of the new fundamental results, but we do not cover all topics fully. Many more details are found in the more comprehensive review in *Annual Review of Fluid Mechanics* (Williamson and Govardhan, 2004). Excellent work has been done by many researchers to bring the fundamentals into practical design codes. There is clearly inadequate full-scale data for fluid–structure interactions in a variety of conditions, including sheared flows in the ocean. VIV behavior at large Re is in need of a parallel effort to see which phenomena in this review remain relevant to full-scale structures, and to discover what new phenomena appear. VIV suppression is important.

There are some important efforts underway to explore phenomena at high Reynolds numbers. Triantafyllou et al. (2003) has described some high $Re \sim 10^6$ experiments, taken from a massive facility in St. Johns, Newfoundland, which indicates the existence of distinct response branches and the 2S and 2P modes, although as yet the key results have not been made public. A further significant result has been presented by Bearman et al. (2001), who have presented excellent agreement between in-line response measurements at $Re \sim 10^4$ and at $Re \sim 10^5$ (the latter made possible in the large Delft delta flume, Netherlands). There was also good agreement for the limited transverse VIV response data at these Re. In essence, we have encouraging signs of agreement between laboratory-scale response with full-scale VIV data, but there is no complete comparison at high Re which is yet to be available in the public domain.

One of the most fundamental questions concerning VIV is, what is the maximum attainable amplitude in VIV of an elastically mounted cylinder? We may also ask, what is the functional relationship between peak amplitudes and mass damping, in the Griffin plot? Surprizingly, neither of these questions has been answered definitively, although there are ongoing efforts to yield precise well-defined data.

What generic characteristics exist for VIV, which carry across from the paradigm of the elastically mounted cylinder, in transverse vibration, to more complex systems? It is fascinating that the response branches for this "simple" paradigm are found similarly for cylinders in XY motion, for flexible cantilevers, for pivoted cylinders, for vibrating cables, and possibly for other systems. The concept of a critical mass has been introduced, whereby the regime of synchronization extends to infinite flow velocity—in a sense the body resonates forever!

Some disagreements apparently persist on VIV problems, for example the "controversy" regarding added mass, although it is not obvious why such controversies continue. There is also debate about whether results from our paradigm, the Y-only free vibration of a cylinder, carry across to two degrees of freedom (XY motion). Fortunately, for the hundreds of papers concerned with the paradigm, the results carry across very well. However, this similarity breaks down for very low vibrating mass.

Further ideas have been developed in the last few years. A recent fundamental contribution is the use of the "effective elasticity" concept to reduce the number of parameters to define the VIV problem for very-small damping (Leonard and Roshko, 2001), also discussed further in Williamson and Govardhan (2004). As the tools of analysis, simulation, and experiment are further sharpened, we may expect more fundamentally new

contributions to emerge, and further universal or generic characteristics to be discovered, which carry across from one VIV system to another, and to regimes of higher Reynolds numbers.

Acknowledgment

We gratefully acknowledge the support from the Ocean Engineering Division of the Office of Naval Research (ONR), monitored by Dr. Tom Swean (ONR Contract no. N00014–95–1–0332).

Appendix A. Nondimensional groups

Mass ratio	m^*	$\frac{m}{\pi\rho D^2 L/4}$
Damping ratio	ζ	$\frac{c}{2\sqrt{k(m+m_A)}}$
Velocity ratio	U^*	$\frac{U}{f_N D}$
Amplitude ratio	A^*	$\frac{y_0}{D}$
Frequency ratio	f^*	$\frac{f}{f_N}$
Streamwise force coefficient	C_X	$\frac{F_X}{\frac{1}{2}\rho U^2 DL}$
Transverse force coefficient	C_Y	$\frac{F_Y}{\frac{1}{2}\rho U^2 DL}$
Reynolds number	Re	$\frac{\rho UD}{\mu}$

Notes regarding these groups:

- We choose here to use f_N as the natural frequency in still water, and correspondingly use ζ as the ratio (structural damping)/(critical damping in water). The frequency f, used in f^*, is the actual body oscillation frequency during induced vibration.
- The added mass, $m_A = C_A m_d$, where $m_d = \pi\rho D^2 L/4$ is the displaced mass of fluid, and where L is the cylinder length. CA is the added mass coefficient for small transverse oscillations in otherwise still fluid, and experiments yield values of $CA \approx 1.0$ to within 5%, supporting the use of the inviscid flow coefficient $CA = 1$. (This CA should not be confused with the transverse force coefficient often measured in phase with the acceleration during flow-induced vibration, which of course is a function of amplitude and frequency of vibration, etc.).

References

Anand, N.M., Torum, A., 1985. Free span vibration of submerged pipelines in steady flow and waves. In: Proceedings of the International Symposium on Separated Flow Around Marine Structures, Trondheim, Norway, pp. 155–199.

Anagnostopoulos, P. (Ed.), 2002. Flow-Induced Vibrations in Engineering Practice. WIT Press, Ashurst, UK.

Angrilli, F., Disilvio, G., Zanardo, A., 1974. Hydroelasticity study of a circular cylinder in a water stream. In: Naudascher, E. (Ed.), Flow Induced Structural Vibrations. Springer, Berlin, pp. 504–512.

Balasubramanian, S., Skop, R.A., Haan, F.L., Szewczyk, A.A., 2000. Vortex-excited vibrations of uniform pivoted cylinders in uniform and shear flow. J. Fluids Struct. 14, 65–85.

Bearman, P.W., 1984. Vortex shedding from oscillating bluff bodies. Annu. Rev. Fluid Mech. 16, 195–222.

Bearman, P.W., Williamson, C.H.K. (Eds.), 1998. Proceedings of the Conference on Bluff Body Wakes and Vortex-Induced Vibrations, Washington, DC, 21–23 June. Cornell University, New York. (Also, in highly segemented form on CD-ROM for the ASME Fluids Engineering Summer Meeting, FEDSM98.)

Bearman, P.W., Johanning, L., Owen, J.C., 2001. Large-scale laboratory experiments on vortex-induced vibration. In: Proceedings of OMAE 2001–the 20th International Conference on Offshore Mechanics and Arctic Engineering, Rio de Janeiro, Brazil, 3–8 June.

Bearman, P.W., Owen, J.C., 1998. Reproduction of bluff-body drag and suppression of vortex shedding by the introduction of wavy separation lines. J. Fluids Struct. 12, 123–130.

Bishop, R.E.D., Hassan, A.Y., 1964. The lift and drag forces on a circular cylinder oscillating in a flowing fluid. Proc. R. Soc. London Ser. A 277, 51–75.

Blackburn, H.M., Govardhan, R.N., Williamson, C.H.K., 2001. A complementary numerical and physical investigation of vortex-induced vibration. J. Fluids Struct. 15.

Blackburn, H., Karniadakis, G.E., Two and three-dimensional simulations of vortex-induced vibration of a circular cylinder, In: Proceedings of the Third International Offshore Polar Engineering Conference, vol. 3, 1993, pp. 715–720.

Blevins, R.D., 1990. Flow-Induced Vibrations. Van Nostrand Reinhold, New York.

Brika, D., Laneville, A., 1993. Vortex-induced vibrations of a long flexible circular cylinder. J. Fluid Mech. 250, 481–508.

Brika, D., Laneville, A., 1995. An experimental study of the aeolian vibrations of a flexible circular cylinder at different incidences. J. Fluids Struct. 9, 371–391.

Carberry, J., Sheridan, J., Rockwell, D.O., 2001. Wake modes of an oscillating cylinder. J. Fluids Struct. 15.

Carberry, J., Sheridan, J., Rockwell, D.O., 2003. Controlled oscillations of a cylinder: a new wake state. J. Fluids Struct. 17, 337–343.

Carberry, J., Sheridan, J., Rockwell, D.O., 2004. Wake states and response branches of forced and freely oscillating cylinder. Eur. J. Mech. B 23, 89–97.

Carberry, J., Sheridan, J., Rockwell, D.O., 2005. Controlled oscillations of a cylinder: forces and wake modes. J. Fluid Mech. 538, 31–69.

Dong, P., Benaroya, H., Wei, T., 2003. Integrating experiments into an energy-based reduced-order model for VIV of a cylinder mounted as an inverted pendulum. J. Sound Vib. 276, 45–63.

Evangelinos, C., Karniadakis, G.E., 1999. Dynamics and flow structures in the turbulent wake of rigid and flexible cylinders subject to vortex-induced vibrations. J. Fluid Mech. 400, 91–124.

Facchinetti, M.L., DeLangre, E., Biolley, F., 2004. Vortex-induced travelling waves along a cable. Eur. J. Mech. B 23, 199–208.

Feng, C.C., 1968. The measurements of vortex-induced effects in flow past a stationary and oscillating circular and D-section cylinders. Master's thesis, University of British Columbia, Vancouver, Canada.

Flemming, F., Williamson, C.H.K., 2003. Vortex-induced vibrations of a pivoted cylinder. J. Fluid Mech. 522, 215–252.

Fujarra, A.L.C., Pesce, C.P., Flemming, F., Williamson, C.H.K., 2001. Vortex-induced vibration of a flexible cantilever. J. Fluids Struct. 15, 651–658.

Gharib, M.R., Leonard, A., Gharib, M., Roshko, A., 1998. The absence of lock-in and the role of mass ratio. In: Bearman, P.W., Williamson, C.H.K. (Eds.), 1998. Proceedings of the conference on Bluff Body Wakes and Vortex-Induced Vibrations, Washington, DC, 21–23 June, Paper No. 24. Cornell University, New York; also Paper FEDSM98-5312 in CD-ROM from ASME.

Gopalkrishnan, R., 1993. Vortex-induced forces on oscillating bluff cylinders. Ph.D. Thesis. MIT, Cambridge, MA.

Govardhan, R., Williamson, C.H.K., 2000. Modes of vortex formation and frequency response for a freely vibrating cylinder. J. Fluid Mech. 420, 85–130.

Govardhan, R., Williamson, C.H.K., 2002. Resonance forever: existence of a critical mass and an infinite regime of resonance in vortex-induced vibration. J. Fluid Mech. 473, 147–166.

Griffin, O.M., 1980. Vortex-excited cross-flow vibrations of a single cylindrical tube. ASME J. Pressure Vessel Technol. 102, 158–166.

Griffin, O.M., Ramberg, S.E., 1974. The vortex street wakes of vibrating cylinders. J. Fluid Mech. 66, 553–576.

Griffin, O.M., Ramberg, S.E., 1976. Vortex shedding from a cylinder vibrating in line with an incident uniform flow. J. Fluid Mech. 75, 257–271.

Griffin, O.M., Ramberg, S.E., 1982. Some recent studies of vortex shedding with application to marine tubulars and risers. Trans. ASME J. Energy Resour. Technol. 104, 2–13.

Griffin, O.M., Skop, R.A., Ramberg, S.E., 1975. The resonant vortex-excited vibrations of structures and cable systems. In: Proceedings of the Seventh Offshore Technology Conference, Houston, TX, OTC Paper 2319.

Gu, W., Chyu, C., Rockwell, D., 1994. Timing of vortex formation from an oscillating cylinder. Phys. Fluids 6, 3677–3682.

Hover, F., Davis, J.T., Triantafyllou, M.S., 1997. Vortex-induced vibration of marine cables: experiments using force feedback. J. Fluids Struct. 11, 307–326.

Hover, F.S., Techet, A.H., Triantafyllou, M.S., 1998. Forces on oscillating uniform and tapered cylinders in crossflow. J. Fluid Mech. 363, 97–114.

Hover, F.S., Tvedt, H., Triantafyllou, M.S., 2001. Vortex-induced vibrations of a cylinder with tripping wires. J. Fluid Mech. 448, 175–195.

Jauvtis, N., Williamson, C.H.K., 2003a. Vortex-induced vibration of a cylinder with two degrees of freedom. J. Fluids Struct. 17, 1035–1042.

Jauvtis, N., Williamson, C.H.K., 2003b. A high-amplitude 2T mode of vortex formation, and the effects of non-harmonic forcing in vortex-induced vibration. Eur. J. Mech. B 23, 107–115.

Jauvtis, N., Williamson, C.H.K., 2003c. The effects of two degrees of freedom on vortex-induced vibration. J. Fluid Mech. 509, 23–62.

Jeon, D., Gharib, M., 2001. On circular cylinders undergoing two-degree-of-freedom forced motions. J. Fluids Struct. 15, 533–541.

Khalak, A., Williamson, C.H.K., 1996. Dynamics of a hydroelastic cylinder with very low mass and damping. J. Fluids Struct. 10, 455–472.

Khalak, A., Williamson, C.H.K., 1997a. Fluid forces and dynamics of a hydroelastic structure with very low mass and damping. J. Fluids Struct. 11, 973–982.

Khalak, A., Williamson, C.H.K., 1997b. Investigation of the relative effects of mass and damping in vortex-induced vibration of a circular cylinder. J. Wind Eng. Ind. Aerodyn. 69–71, 341–350.

Khalak, A., Williamson, C.H.K., 1999. Motions, forces and mode transitions in vortex-induced vibrations at low mass-damping. J. Fluids Struct. 13, 813–851.

Kim, W.J., Perkins, N.C., 2002. Two-dimensional vortex induced vibration of cable suspensions. J. Fluids Struct. 16, 229–245.

King, R., 1974. Vortex-excited oscillations of a circular cylinder in steady currents. In: Proceedings of the Offshore Technology Conference, Paper OTC 1948.

Koumoutsakos, P., Leonard, A., 1995. High-resolution simulations of the flow around an impulsively started cylinder using vortex methods. J. Fluid Mech. 296, 1–38.

Leonard, A., Roshko, A., 2001. Aspects of flow-induced vibration. J. Fluids Struct. 15, 415–425.

Leweke, T., Bearman, P.W., Williamson, C.H.K. (Eds.), 2001. Bluff body wakes and vortex-induced vibration. J. Fluids Struct. 15 (3–4), 669pp. (special issue).

Leyva, J., Rockwell, D.O., Jauvtis, N., Williamson, C.H.K., 2007. A comparative study of XY vortex-induced vibration of a circular cylinder. J. Fluids Struct., in preparation.

Lighthill, J., 1979. Waves and hydrodynamic loading. In: Proceedings of the Second International Conference on the Behavior of Off-Shore Structures, vol. 1, BHRA Fluid Engineering, Cranfield, Bedford, England, pp. 1–40.

Lighthill, J., 1986. Fundamentals concerning wave loading on offshore structures. J. Fluid Mech. 173, 667–681.

Lin, J.C., Rockwell, D., 1996. Force identification by vorticity fields: techniques based on flow imaging. J. Fluids Struct. 10, 663–668.

Lucor, D., Imas, L., Karniadakis, G.E., 2001. Vortex dislocations and force distribution of long flexible cylinders subjected to sheared flows. J. Fluids Struct. 15.

Marcollo, H., Hinwood, J.B., 2002. Vortex-induced vibration of a long flexible cylinder in uniform flow with both forcing and response. In: Hourigan, K., Leweke, T., Thompson, M.C., Williamson, C.H.K. (Eds.), Proceedings of BBVIV-3 Conference on Bluff Body Wakes and Vortex-Induced Vibrations, 17–20 December 2002, Port Douglas, Australia, pp. 219–223.

Mercier, J.A., 1973. Large amplitude oscillations of a circular cylinder in a low speed stream. Ph.D. Thesis, Stevens Institute of Technology, Hoboken, NJ.

Moe, G., Overvik, T., 1982. Current-induced motions of multiple risers. In: Proceedings of BOSS-82, Behaviour of Offshore Structures, vol. 1, Cambridge, MA, USA.

Moe, G., Wu, Z.J., 1990. The lift force on a cylinder vibrating in a current. ASME J. Offshore Mech. Arctic Eng. 112, 297–303.

Naudascher, E., 1987. Flow-induced streamwise vibrations of structures. J. Fluids Struct. 1, 265–298.

Naudascher, E., Rockwell, D., 1994. Flow-Induced Vibrations: An Engineering Guide. Balkema, Rotterdam, Netherlands.

Newman, D.J., Karniadakis, G.E., 1996. Simulations of flow over a flexible cable: comparison of forced and flow-induced vibration. J. Fluids Struct. 10, 439–453.

Newman, D.J., Karniadakis, G.E., 1997. Simulations of flow past a freely vibrating cable. J. Fluid Mech. 344, 95–136.

Noca, F., Shiels, D., Jeon, D., 1999. A comparison of methods for evaluating time-dependent fluid dynamic forces on bodies, using only velocity fields and their derivatives. J. Fluids Struct. 13, 551–578.

Ongoren, A., Rockwell, D., 1988a. Flow structure from an oscillating cylinder. Part 1. Mechanisms of phase shift and recovery in the near wake. J. Fluid Mech. 191, 197–223.

Ongoren, A., Rockwell, D., 1988b. Flow structure from an oscillating cylinder. Part 2. Mode competition in the near wake. J. Fluid Mech. 191, 225–245.

Owen, J.C., Bearman, P.W., Szewczyk, A.A., 2001. Passive control of VIV with drag reduction. J. Fluids Struct. 15, 597–606.

Parkinson, G.V., 1989. Phenomena and modelling of flow-induced vibrations of bluff bodies. Prog. Aerosp. Sci. 26, 169–224.

Pesce, C.P., Fujarra, A.L.C., 2000. Vortex-induced vibrations and jump phenomenon: experiments with a clamped flexible cylinder in water. Int. J. Offshore Polar Eng. 10, 26–33.

Sarpkaya, T., 1978. Fluid forces on oscillating cylinders. ASCE J. Waterway Port Coast. Ocean Div. 104, 275–290.

Sarpkaya, T., 1979. Vortex-induced oscillations. ASME J. Appl. Mech. 46, 241–258.

Sarpkaya, T., 1993. Offshore hydrodynamics. ASME J. Offshore Mech. Arctic Eng. 115, 2–5.

Sarpkaya, T., 1995. Hydrodynamic damping, flow-induced oscillations, and biharmonic response. ASME J. Offshore Mech. Arctic Eng. 117, 232–238.

Sarpkaya, T., 2001. On the force decompositions of Lighthill and Morison. J. Fluids Struct. 15, 227–233.

Scruton, C., 1965. On the wind-excited oscillations of towers, stacks and masts. In: Proceedings of the Symposium Wind Effects on Buildings and Structures, vol. 16, HMSO, London, pp. 798–836.

Sheridan, J., Carberry, J., Lin, J.C., Rockwell, D., 1998. On the near wake topology of an oscillating cylinder. J. Fluids Struct. 12, 215–220.

Skop, R.A., 1974. On modelling vortex-excited oscillations. NRL Memo. Rep. 2927.

Skop, R.A., Balasubramanian, S., 1997. A new twist on an old model for vortex-excited vibrations. J. Fluids Struct. 11, 395–412.

Skop, R.A., Griffin, O.M., 1973. An heuristic model for determining flow-induced vibrations of offshore strcutures. In: Proceedings of the Fifth Offshore Technology Conference, Houston, TX, OTC Paper 1843.

Skop, R.A., Luo, G., 2001. An inverse–direct method for predicting the vortex-induced vibrations of cylinders in uniform and nonuniform flows. J. Fluids Struct. 15, 867–884.

Staubli, T., 1983. Calculation of the vibration of an elastically mounted cylinder using experimental data from forced oscillation. ASME J. Fluids Eng. 105, 225–229.

Stokes, G.G., 1851. On the effect of the internal friction of fluids on the motion of pendulums. Trans. Cambridge Philos. Soc. 9, 8–106.

Sumer, B.M., Fredsφe, J., 1997. Hydrodynamics Around Cylindrical Structures. World Scientific, Singapore.

Techet, A.H., Hover, F.S., Triantafyllou, M.S., 1998. Vortical patterns behind a tapered cylinder oscillating transversely to a uniform flow. J. Fluid Mech. 363, 79–96.

Tombazis, N., Bearman, P.W., 1997. A study of three-dimensional aspects of vortex shedding from a bluff body with a mild geometric disturbance. J. Fluid Mech. 330, 85–112.

Triantafyllou, M.S., Hover, F.S., Yue, D.K.P., 2003. Vortex-induced vibrations of slender structures in shear flow: a review. In: Benaroya, H., Wei, T. (Eds.), Proceedings of the IUTAM Symposium on Coupled Fluid–Structure Interaction using Analysis, Computations and Experiments, Rutgers, NJ, Paper I-6.

Triantafyllou, M.S., Grosenbaugh, M.A., 1995. Prediction of vortex-induced vibrations in sheared flows. In: Bearman, P.W. (Ed.), Flow-Induced Vibration. Balkema, Rotterdam, Netherlands, pp. 73–82.

Vandiver, J.K., 1993. Dimensionless parameters important to the prediction of vortex-induced vibration of long flexible cylinders in ocean currents. J. Fluids Struct. 7, 423–455.

Vandiver, J.K., 2003. SHEAR 7 User Guide. Department of Ocean Engineering, MIT, Cambridge, MA.

Vandiver, J.K., Jong, J.-Y., 1987. The relationship between in-line and cross-flow vortex-induced vibration of cylinders. J. Fluids Struct. 1, 381–399.

Vickery, B.J., Watkins, R.D., 1964. Flow-induced vibrations of cylindrical structures. In: Silvester, R. (Ed.), Proceedings of the First Australian Conference on Hydraulics and Fluid Mechanics. Pergamon, New York, pp. 213–241.

Vikestad, K., Vandiver, J.K., Larsen, C.M., 2000. Added mass and oscillation frequency for a circular cylinder subjected to vortex-induced vibrations and external disturbance. J. Fluids Struct. 14, 1071–1088.

Voorhees, A., Wei, T., 2002. Three-dimensionality in the wake of a surface piercing cylinder mounted as an inverted pendulum. In: Hourigan, K., Leweke, T., Thompson, M.C., Williamson, C.H.K. (Eds.), Proceedings of BBVIV-3 Conference on Bluff Body Wakes and Vortex-Induced Vibrations, 17–20 December 2002, Port Douglas, Australia, pp. 133–136.

Weiss, L.G., Szewczyk, A.A., 2000. An experimental investigation of some three-dimensional effects of pivoted circular cylinders. In: Ziada, S., Staubli, T. (Eds.), Flow Induced Vibration. Balkema, Rotterdam, Netherlands, pp. 75–83.

Willden, R.H.J., Graham, J.M.R., 2001. Numerical prediction of VIV on long flexible circular cylinders. J. Fluids Struct. 15, 659–669.

Williamson, C.H.K., 1992. The natural and forced formation of spot-like L-structures caused by vortex dislocations in wake transition. J. Fluid Mech. 243, 393–441.

Williamson, C.H.K., Govardhan, R., 2004. Vortex-induced vibrations. Annu. Rev. Fluid Mech. 36, 413–455.

Williamson, C.H.K., Roshko, A., 1988. Vortex formation in the wake of an oscillating cylinder. J. Fluids Struct. 2, 355–381.

Wooton, L.R., Warner, M.H., Sainsbury, R.N., Cooper, D.H., 1972. Oscillations of piles in marine structures. A resume of full-scale experiments at Immingham. CIRIA Tech. Rep. 41.

Zdera, R., Turan, Ö.F., Havard, D.G., 1995. Towards understanding galloping: near-wake study of oscillating smooth and stranded circular cylinders in forced motion. Exp. Therm. Fluid Sci. 10, 28–43.

Zdravkovich, M.M., 1981. Review and classification of various aerodynamic and hydrodynamic means for suppressing vortex shedding. J. Wind Eng. Ind. Aerodyn. 7, 145–189.

Zdravkovich, M.M., 1982. Modification of vortex shedding in the synchronization range. ASME J. Fluids Eng. 104, 513–517.